



Characterization and Optimization of Crustacean Shell-derived Activated Carbon for Wastewater Treatment Applications

Akomah, Uchechi ^a, Nwaogazie, Ify L. ^{b*}
and Akaranta, Onyewuchi ^c

^a World Bank Africa Centre of Excellence in Oilfields Chemicals Research, University of Port Harcourt, Choba, Rivers State, Nigeria.

^b Department of Civil and Environmental Engineering, University of Port Harcourt, Choba, Rivers State, Nigeria.

^c Department of Industrial Chemistry, University of Port Harcourt, Choba, Rivers State, Nigeria.

Authors' contributions

This work was carried out in collaboration among all authors. All authors read and approved the final manuscript.

Article Information

DOI: <https://doi.org/10.9734/ijecc/2024/v14i104486>

Open Peer Review History:

This journal follows the Advanced Open Peer Review policy. Identity of the Reviewers, Editor(s) and additional Reviewers, peer review comments, different versions of the manuscript, comments of the editors, etc are available here:

<https://www.sdiarticle5.com/review-history/123527>

Original Research Article

Received: 19/07/2024

Accepted: 22/09/2024

Published: 30/09/2024

ABSTRACT

Comparative studies of the Surface Chemistry, morphology, and physicochemical properties of crustacean shells activated chemically using acid (H₂SO₄) and base (KOH) were investigated. Following the activation, samples of acid and base activated Periwinkle shells (PSAAC and PSBAC), Clam shells (CSAAC and CSBAC), whelk shells (WSAAC and WSBAC), and a 1:1

*Corresponding author: E-mail: ifynwaogazie@yahoo.com;

Clam/Whelk composite Shells (CWSAAC and CWSBAC) were obtained. The properties investigated were moisture content, specific gravity, surface area, porosity, ash content, carbon yield, fixed carbon, FTIR, and SEM-EDX. The findings demonstrate the good physicochemical qualities of activated carbons made from Periwinkle, Clams, Whelks, and a Clam/Whelk composite by acid and base activation for the treatment of wastewater. Among them, the Clam acid-activated carbon (CSAAC) demonstrated exceptional physicochemical qualities with a surface area of 1277 m²/g, moisture content of 1.4%, ash content of 8.3%, carbon yield of 87%, and fixed carbon of 63.7%. On the other hand, the Clam Shell Base-Activated Carbon (CSBAC) exhibited a greater porosity of 0.88, indicating that it could be a more efficient option for adsorption in wastewater treatment. Both base- and acid-activated carbons generally showed modest ash contents; however, at 12.3%, Whelk Shell Base-Activated Carbon (WSBAC) had the highest ash concentration. The bulk densities of acid- and base-activated carbons were almost identical. The bulk densities, from highest to lowest, were CSBAC > CSAAC > CWSBAC > CWSAAC > PSBAC > PSAAC > WSBAC > WSAAC, with values ranging from 0.687 g/cm³ to 0.454 g/cm³. The porosity of the samples, ranked in descending order, was CSBAC > PSBAC > CSAAC > CWSAAC > PSAAC = CWSBAC > WSAAC > WSBAC, with values from 0.88 to 0.59. FTIR and SEM-EDX indicated that all samples were successfully converted to activated carbon. The results of this study demonstrate that it is possible to chemically activate crustacean shells using either an acid or a base without sacrificing the effectiveness of the activated sample that is produced, which can be used to remove adsorbates from wastewater samples. As a result, the selection of activation is widened since the natural abundance of precursors exists.

Keywords: Surface chemistry; morphology; crustacean shells; acid activation; base activation; wastewater treatment.

1. INTRODUCTION

Activated carbon (AC) has been globally recognized as the oldest, most widely used, and popular adsorbent in the water and wastewater treatment industries [1]. AC is “char”, which has been subjected to a reaction with gases and/or chemicals during or after carbonization to increase its adsorption capacities. [2] described char as “a carbonization product of a natural or synthetic organic material, which has not passed through a fluid stage during carbonization”. AC refers to a wide range of carbonized materials with a high degree of porosity and high surface area [3].

Due to the high cost of available commercial AC, various studies focus on developing new low-cost AC with properties comparable to that of commercial ones [4]. This has given rise to extensive studies on low-cost adsorbents ranging from plant seeds, stems, and husks to animal biomass. Carbon adsorbents derived from biomass (agricultural and household residues) have been widely used in the removal of hazardous substances from the environment due to their distinctive qualities of large internal surface area, mechanical integrity, and regeneration [5] The choice of precursor for low-cost activated carbon should be preferable freely available, inexpensive, and nonhazardous for nature [6].

[7] reported that an estimated global quantity of crustacean shell waste discarded ranges between 6 and 8 million tonnes every year. Due to the immense nature of crustacean shells, they occupy valuable space when discarded in landfills, thereby potentially necessitating the formation of new landfill sites, which can have substantial economic and environmental implications. Recent advancement in Research has found that Chitin, found in shells is an invaluable resource as it accounts for its versatility for use in various industries. It is estimated that approximately 80% of chitin production comes from crustacean shells [8].

Chitin is the second most abundant natural biopolymer after cellulose and is widely used due to its abundance, renewability, and low cost [8]. These have become a new source of raw material for various industries that have found value in the otherwise waste product. The utilization of waste shells as a renewable and cheap alternative to traditional materials in industries which include the cosmetic, food, and feed industries as well as materials for various applications, including heterogenous catalysts, blended cement manufacture, concrete aggregate, ceramics and plastics additives, biofilter medium, and biomedical applications are available in literature [9,10].

Nigeria has a coastline of 853km which lies between Latitude 4° 10' to 6°20'N and longitude 2° 45' to 8° 5' E which stretches from the Western border with the Republic of Benin to the eastern border with the Cameroon Republic [11]. This vast coastline offers a wide range of crustaceans Indigenous to the country including Periwinkles (*Tympanotamus fuscatus*), West African Clams (*Galatea paradoxa*), and Whelks (*Buccium Undatum*).

These crustacean shells have also been used as renewable, energy-efficient, cost-effective, and sustainable alternative materials. These include the use of oyster and pyramidella shells as heterogeneous catalysts for the microwave-assisted biodiesel production from *Jatropha curcas* oil [10]; the use of periwinkle shells in carburization, specifically in improving the surface hardness of low carbon steel contributing to the improvement of mechanical properties in mild steel [12] and the use of ground periwinkle shell as a filler in brake friction [13]. Chitin can be transformed into biochar through pyrolysis, and the resulting chitin-biochar has potential applications in water treatment [8].

AC has been utilized as an adsorbent material for the removal of target contaminants from aqueous environments as well as in solid-gas experiments, to measure the adsorption capacities and selectivity toward Carbon (IV) oxide [14]. It is expected that more research will explore their potential as very useful engineering materials. This study therefore aims to compare the Morphology, elemental analysis, functional groups, and Physicochemical properties of acid and base-activated crustacean shells as effective low-cost adsorbents for wastewater treatment.

2. MATERIALS AND METHODS

2.1 Sample Collection, Preparation, and Carbonization

Periwinkle shells (*Tympanotamus fuscatus*), West African Clamshells (*Galatea paradoxa*), and Whelk shells (*Buccium Undatum*) were purchased from Town Market in Borokiri, Port Harcourt, Rivers State in Nigeria. They were soaked with a cleansing agent and warm water for four days to remove dust, remnant organic particles as well as soluble impurities. The shells were thoroughly washed with tap water with continuous agitation to loosen remnant

impurities. The shells were sun-dried for three days before carbonization at 450°C for 3 hours and then pulverized to powder. The Composite was prepared before chemical activation. The samples were divided into two equal parts for chemical activation by acid and base.

2.2 Chemical Activation

(i) **Acid Activation:** The samples were soaked in 0.5 M of H₂SO₄ and mixed until a paste was formed then heated in a muffle furnace for 750°C for 2 hours. The resultant sample was then cooled, and washed with deionized water to a pH of 6. The samples were then dried in the oven at 105°C for 6 hours and stored in air-tight containers.

(ii) **Base Activation:** The samples were soaked in 0.5 M KOH and mixed until a paste was formed then heated in a muffle furnace for 650° for 2 hours. The resultant sample was then cooled, and washed with deionized water to a pH of 6. The samples were then dried in the oven at 105°C for 6 hours and stored in air-tight containers.

2.3 Surface Chemistry and Morphology Determination

Attenuated Total Reflectance Fourier Transform Infrared Spectroscopy (ATR-FTIR) was performed using Agilent Technologies Cary 630 FTIR Cary630 ZnSe. PART NO: - G8043 64002, Model NO: - MY19322004. The samples spectra were collected by placing the samples onto the ATR crystal and applying pressure to ensure good contact with the crystal. The spectra were then collected by shining an infrared beam onto the crystal and measuring the reflected light as a function of wavelength. The collected spectra were typically processed using software to remove any remaining baseline drift or noise.

Scanning electron microscopy-energy dispersive X-ray analysis was performed using a PHENOM PRO X Serial no: MVE0224651193 Model no: 800-07334. The samples were mounted on stubs with adhesive carbon and coated in 20 nm Carbon with a QUORUM Q150R ES mini sputter coater, and then analyzed with a Phenom PRO-X SEM equipped with an Oxford XMax 50 Silicon Drift Energy Dispersive X-ray detector at 15KV under high vacuum.

2.3.1 Determination of physicochemical properties

2.3.1.1 Carbon yield

Carbon yield for the activated carbon samples was determined using the [15] technique. This technique involved measuring the weight of each carbon sample before and after carbonization and the yield calculated using Equation 1

$$\text{Carbon Yield} = \frac{W_f}{W_o} \times 100 \quad (1)$$

Where: W_f = mass of carbon retrieved from the furnace

W_o = mass of oven-dried sample before carbonization

2.3.1.2 Moisture Content

The moisture content was measured using the air oven method. A known mass of each activated carbon sample was weighed and dried in an oven at a temperature of 105°C for 6 hours and the samples were re-weighed after drying and the new weight recorded. The moisture content was then calculated as the ratio of the change in weight to the original weight expressed as a percentage. This is represented in Equation 2.

$$\frac{W_o - W_d}{W_o} \times 100\% \quad (2)$$

Where:

W_o = original weight (g)

W_d = weight after drying (g).

The test was performed twice on each activated carbon sample and the average value was obtained.

2.3.1.3 Ash content

The ash content was determined using the standard test method for ash content [16]. A crucible was pre-heated in a furnace to about 500°C and then cooled in a desiccator. 1.0g of the activated sample was transferred into the crucible and re-weighed (oven-dry weight). The crucible and sample were then placed in the furnace and the temperature was raised to 630°C for 6 hours. The sample was then removed and allowed to cool in a desiccator to room temperature and re-weighed (ash weight). The

Ash content of the sample was calculated from Equation 3.

$$\% \text{ Ash Content} = \frac{\text{Ash weight}}{\text{Oven dry weight}} \times 100 \quad (3)$$

2.3.1.4 Specific surface area

The specific surface area of the adsorbent was estimated according to the Sear method [17]. About 1.5g of each prepared adsorbent was mixed with 30 g NaCl and dissolved in 100 mL of distilled water using a 250 mL conical flask. The mixtures were stirred for 5 minutes. Then, the pH of solution was adjusted to 4 by the addition of HCL. The solution was then titrated by 0.1 M NaOH until pH of the solution attained a pH to 9. The volumes of NaOH required to change pH value from 4 to 9 were recorded. The specific surface area of sample was found using Equation 4:

$$\text{specific surface area (S)} \text{ (m}^2/\text{g)} = 32V - 25 \quad (4)$$

where V is the volume of 0.1 M NaOH required to raise the pH from 4.0 to 9.0.

2.3.1.5 Bulk density

The bulk density was measured by utilizing the method of [18]. A measuring centrifuge tube of 10 cm³ volume was first zeroed on the weighing balance. The lump-free sample of each activated carbon of known weight was then taken and poured into the measuring centrifuge tube to the 10 cm³ mark tapping the cylinder for 1 to 2 minutes to ensure no void was created. The weight was then noted and recorded. The bulk density was then calculated using the Equation 5

$$\text{Bulk Density} = \frac{\text{Weight of carbon (g)}}{\text{Volume of dry sample (cm}^3\text{)}} \quad (5)$$

2.3.1.6 Specific gravity

A pycnometer was used for the determination of the specific gravity of the activated carbon samples. The mass of the empty pycnometer (M_1) was found using a weighing balance. Then, a sample of oven-dried AC was placed inside and the combined mass (M_2) was found. Water was then added to the activated carbon and agitated to remove all air pockets after which the pycnometer filled up and its mass (M_3) was measured. Finally, the pycnometer was emptied, cleaned, and filled with water and its new mass (M_4) was found. The specific gravity, G_s was calculated from Equation 6.

$$Gs = M_2 - M_1 / (M_2 + M_4) - (M_1 + M_3) \quad (6)$$

2.3.1.7 Porosity

Porosity or void fraction is a measure of the void spaces in the activated sample, and is a fraction of the volume of voids over the total volume, between 0 and 1, or as a percentage between 0% and 100%. The porosity of the activated samples was calculated using Equation 7

$$n = \frac{(1-p) / \rho_w G_s}{1+w} \quad (7)$$

Where: n = Porosity

ρ = Bulk density of Activated Carbon sample
 ρ_w = Density of water,
 G_s = Specific gravity of Activated Carbon sample = Moisture content.

$$\text{Fixed Carbon} = 100 - (\% \text{ Ash} + \% \text{ Moisture} + \% \text{ volatile matter}) \quad (8)$$

3. RESULTS AND DISCUSSION

The results of the research carried out on the comparative studies of the surface chemistry, morphology, and physicochemical properties of acid and base chemically activated carbon from crustacean shells have been carefully detailed in Tables 1-5 and Figs. 1-6.

3.1 Surface Chemistry and Morphology

FT-IR analysis was performed to identify the functional groups present on the surface of the activated carbons. The FTIR spectra obtained for the prepared acid- and base-treated activated carbon are presented in Figs. 1 and 2 respectively. The spectra data for acid-activated and base-activated samples are summarized in

Tables 1 and 2, respectively. Acid-activated samples exhibited prominent absorption bands corresponding to O-H, C-H, C=O, and C-O groups, indicating the presence of hydroxyl, aliphatic, ester, and carboxyl groups.

Close observation of the spectra of the acid-treated samples, three prominent absorption bands appeared in the functional group domain at ca. 3540, 3394, 1797, and 1616 cm^{-1} which were assigned to O-H, C-H, esters C=O, and amides C=O groups respectively for CSAAC. These bands were observed to occur in similar positions in the spectra of PSAAC, WSAAC, and CWSAAC with only slight bathochromic or hypsochromic shifts which is an indication of similarity in the surface functionality of these materials. Similarly, the bands occurring in the spectrum of CSAAC at 1150, 1398, 873, and 713 cm^{-1} which have been attributed to C-O, C-O-C, M-O, and the aromatic C-H bending vibrations respectively were observed in similar regions in the other acid-treated samples. This evidence further rationalizes the similarity in these materials. The findings herein conform with those of previous studies for similar kinds of materials [19-21].

Base-activated samples showed similar functional groups, with slight variations in absorption band intensities and positions, reflecting differences in surface chemistry due to the activating agent. Furthermore, the spectra of the base-modified samples showed the same absorption bands in similar domains to those of the acid-treated materials with only two striking distinctions. Firstly, the peak intensities of the O-H, C-H, and C-O vibrations drastically decreased in their spectra which may be credited to the treatment of these materials with potassium hydroxide. Secondly, the peak associated with the amide C=O vibration in the spectra of the acid-treated

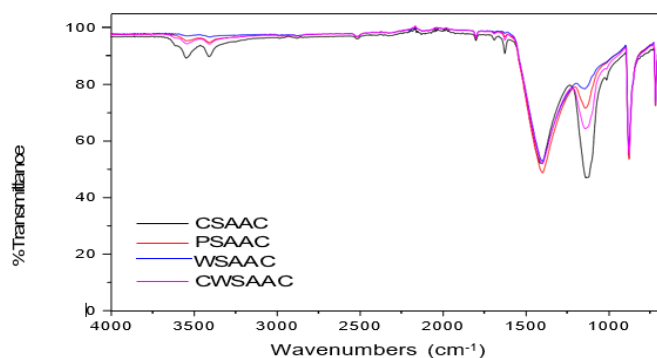


Fig. 1. Stacked FT-IR spectra of acid-treated activated carbon

Table 1. FT-IR spectra data of the acid-activated crustacean shells

Sample/ band (cm ⁻¹)	O-H	C-H	C=O	C-O	C-O-C	M-O	Ar-H
CSAAC	3540	3394	1797; 1616	1122	1398	873	713
PSAAC	3540	3394	1789; 1624	1135	1389	864	704
WSAAC	3553	3398	1797; 1620	1135	1393	869	713
CWSAAC	3550	3398	1793; 1616	1126	1397	869	713

Table 2. FT-IR spectra data of the base-activated crustacean shells

Sample/ band (cm ⁻¹)	O-H	C-H	C=O	C-O	C-O-C	M-O	Ar-H
CSBAC	3553	3345	1797	1122	1398	873	713
PSBAC	3518	3358	1789	1135	1389	864	704
WSBAC	3576	3389	1793	1135	1393	869	713
CWSBAC	3523	3336	1789	1126	1397	869	713

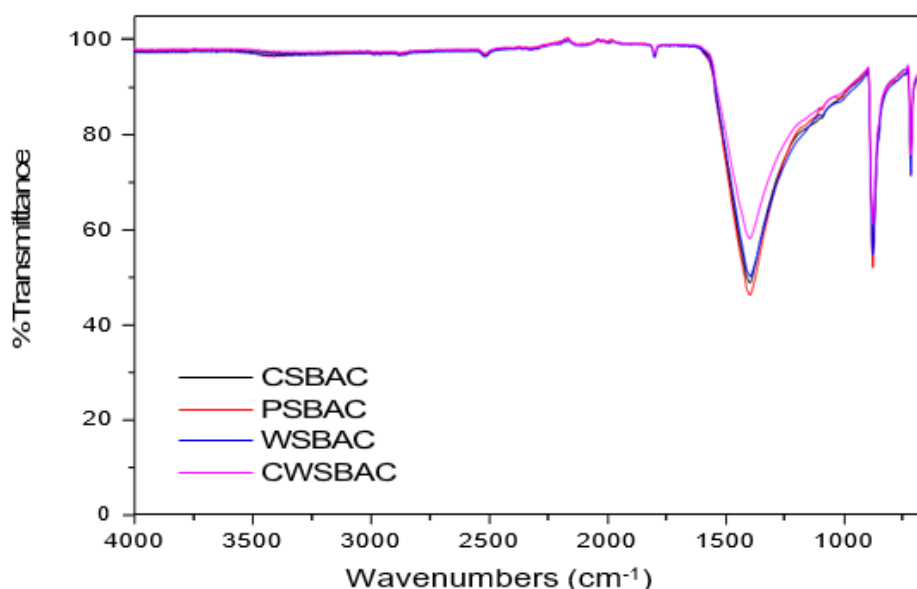


Fig. 2. Stacked FT-IR spectra of base-treated activated carbons

samples is completely missing in the spectra of the base-treated materials. This observation can also be ascribed to the effect of chemical treatment by potassium hydroxide [22].

The SEM image for acid-activated samples in Figure 3 shows that the activated carbon is characterized by surface heterogeneity and varied structures with a large number of pores and pore sizes. This is per findings from [23] that indicated that activated samples with a large number of pores and pore sizes and high surface areas displayed high adsorption capacity and were therefore good activated carbon.

The SEM image for base-activated carbons in Figure 4 indicated a broadly opened pore structure, which indicates well-developed

micropores. This conforms with activation with Potassium Hydroxide (KOH) which produces well-defined micropores that make the activated sample display high adsorption capacity [24]. When the micrographs from the two different sets of samples are compared, a difference in particle size and shape is observed. The differences in particle size and shape observed on the surface of activated carbons may be due to depolymerization and the release of volatile substances from organic substances during the carbonization process and chemical treatments [25]; [26,27]. Interestingly, the surface morphology of the acid-treated materials; CSAAC, PSAAC, WSAAC, and CWSAAC appeared to be similar but distinct from those of their base-treated analogues. Similarly, the micrographs of the CSBAC, PSBAC, WSBAC, and CWSBAC

showed similar features in their surface morphology but at variance with those of acid-modified samples. This observation is in concomitance with the results from FTIR studies which suggest a significant similarity in the surface composition of each set of materials.

Energy dispersive X-ray (EDX) analysis of the treated activated carbon materials was performed to estimate the composition of various elements present in the adsorbents. Tables 3 and 4 provide the atomic and weight concentrations of oxygen (O) and calcium (Ca) in the samples for both the acid and base-activated carbon respectively. Thus, the elemental analysis confirmed the presence of Ca and O in all the materials under investigation. It can be observed that the calcium weight percentage is high in all the treated activated carbons as a result of activation and mineralization with a calcium-to-oxygen weight concentration ratio of 1:1 in all the samples [28,29]. The results indicated a significant presence of calcium oxide (CaO) across all samples, which contributes to the porosity and adsorption capacity of the activated carbons. Acid-activated samples, as presented in

Table 3, showed higher atomic concentrations of oxygen compared to calcium, with CSAAC having the highest oxygen concentration at 78.16 cm^{-1} . Conversely, base-activated samples, detailed in Table 4, demonstrated a more balanced ratio of oxygen and calcium, with CSBAC showing an oxygen concentration of 61.77 cm^{-1} and calcium at 38.23 cm^{-1} . Consequently, the EDX analysis proved the presence of calcium oxide in the activated carbons. As CaO is a strong dehydrating agent, it adsorbs water from surroundings, thus increasing the porosity of the treated activated materials [29] as observed in the SEM studies.

3.2 Carbon Yield

The results from Table 5 showed a high carbon content ranging from 71.6 to 87%. Fig. 5 presents the carbon yield percentages of the activated samples. High product yield difference is a result of the origin of carbon material and activation processes [30]. A good activated carbon should present a carbon yield of 60 to 98% [1].

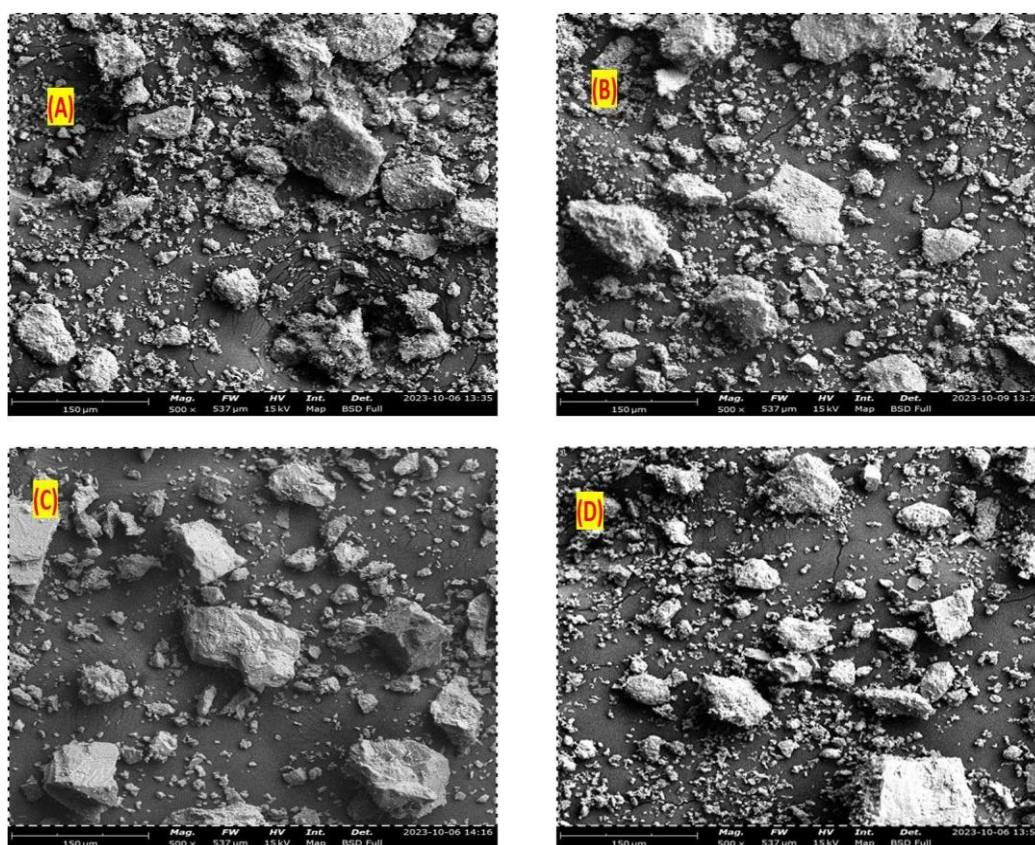


Fig. 3. SEM Micrographs (at 150 μm) of CSAAC (A), PSAAC (B), WSAAC (C), and CWSAAC (D)

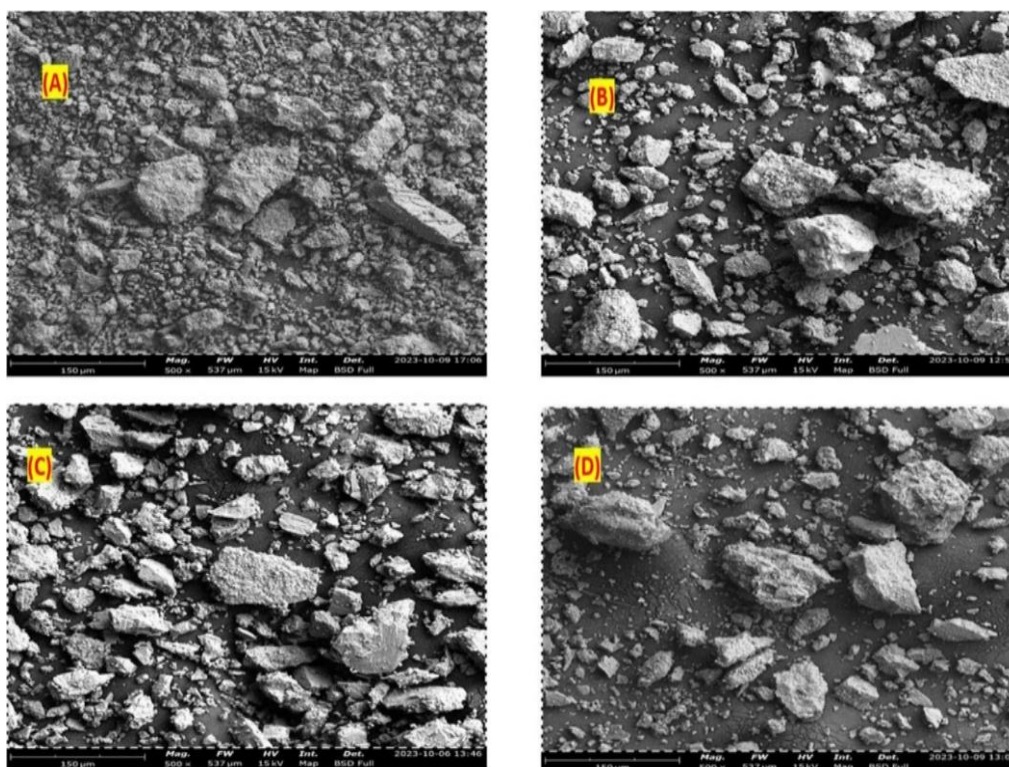


Fig. 4. SEM Micrographs (at 150 μm) of CSBAC (A), PSBAC (B), WSBAC (C), and CWSBAC (D)

The acid-activated samples presented higher carbon yields compared to the base-activated samples. The highest carbon yield was observed in CSAAC at 87%, while WSBAC had the lowest at 71.6%. The high carbon yield is similar to the findings of [31] with a 95% carbon yield from activated crustacean shells. A high carbon content value is desired to achieve a high surface area because as the carbon content of the activated carbon increases, the surface area also increases [1]. A higher carbon yield indicates a greater conversion of raw material into activated carbon, which is desirable for effective adsorption.

3.3 Fixed Carbon

Proximate analysis was used to calculate the fixed carbon content in the various activated samples by utilizing the % ash and moisture content derived from the analysis. It indicates the composition of the biomass regarding the moisture content, volatile matters, ash content, and fixed carbon. [32] noted the mathematical derivation of fixed carbon content and this is expressed in Equation 8.

The fixed carbon content, illustrated in Fig. 6, ranged from 52.8% to 63.7%. Acid-activated samples had slightly higher fixed carbon contents than the base-activated samples, except for WSAAC showing a low value at 53.7%. Among the base-activated samples, CSBAC had the highest fixed carbon content at 62.1%. High fixed carbon content is indicative of greater carbonization and less volatile matter, enhancing the adsorbent's stability and performance.

3.4 Moisture Content

The moisture content of the activated samples is illustrated in Fig. 5. The results indicated that the percentage moisture content ranged from 1.4% to 2.4%. This is in conformance with the results [33] obtained on the low moisture content of crustacean shells. The acid-activated samples (PSAAC, CSAAC, WSAAC, CWSAAC) generally exhibited lower moisture content than the base-activated samples (PSBAC, CSBAC, WSBAC, CWSBAC). Specifically, CSAAC and PSAAC had the lowest moisture content at 1.4%, while WSBAC had the highest at 2.4%. A lower moisture content is preferable as it reduces the adsorbent's dilution effect, enhancing its adsorption efficiency.

Table 3. Elemental analysis of the acid-activated crustacean shells by EDX

Sample/ band (cm ⁻¹)	Element	Atomic concentration	Weight concentration
CSAAC	O	78.16	58.83
	Ca	21.84	41.17
PSAAC	O	67.37	45.18
	Ca	32.63	54.82
WSAAC	O	74.43	53.75
	Ca	25.57	46.25
CWSAAC	O	75.50	55.15
	Ca	24.50	44.85

Table 4. Elemental analysis of the base-activated crustacean shells by EDX

Sample/ band (cm ⁻¹)	Element	Atomic concentration	Weight concentration
CSBAC	O	61.77	39.21
	Ca	38.23	60.79
PSBAC	O	70.97	49.39
	Ca	29.03	50.61
WSBAC	O	71.45	49.97
	Ca	28.55	50.03
CWSBAC	O	74.34	53.63
	Ca	25.66	46.37

Table 5. Physicochemical characteristics of chemical activated carbons of crustacean shells

Parameter/Sample	PSAAC	CSAAC	WSAAC	CWSAAC	PSBAC	CSBAC	WSBAC	CWSBAC
% Moisture	1.4	1.4	2.3	1.6	1.8	2.0	2.4	1.8
% Ash	7.9	8.3	11.8	9.8	8.9	9.3	12.3	9.9
% Carbon Yield	86.2	87	72.1	86.8	84.2	85.2	71.6	86.3
% Fixed Carbon	60.2	63.7	53.7	60.8	61.8	62.1	52.8	59.8
Specific Surface Area (m ² /g)	1193	1277	960	1256	1275	1288	986	1270
Bulk Density (g/cm ³)	0.502	0.653	0.454	0.530	0.524	0.687	0.476	0.543
Specific Gravity	1.27	2.07	0.97	1.98	1.12	2.01	0.91	1.91
Porosity	0.80	0.83	0.62	0.81	0.86	0.88	0.59	0.80

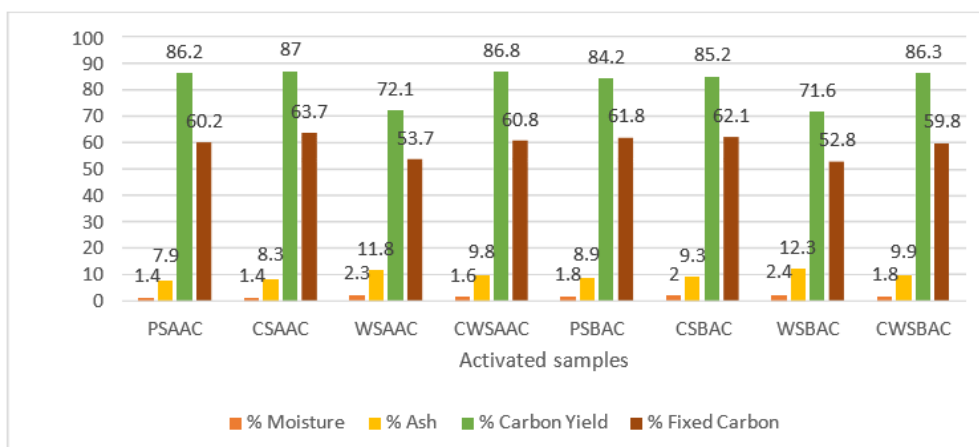


Fig. 5. Comparison between physicochemical properties of acid-activated carbon and base-activated carbon

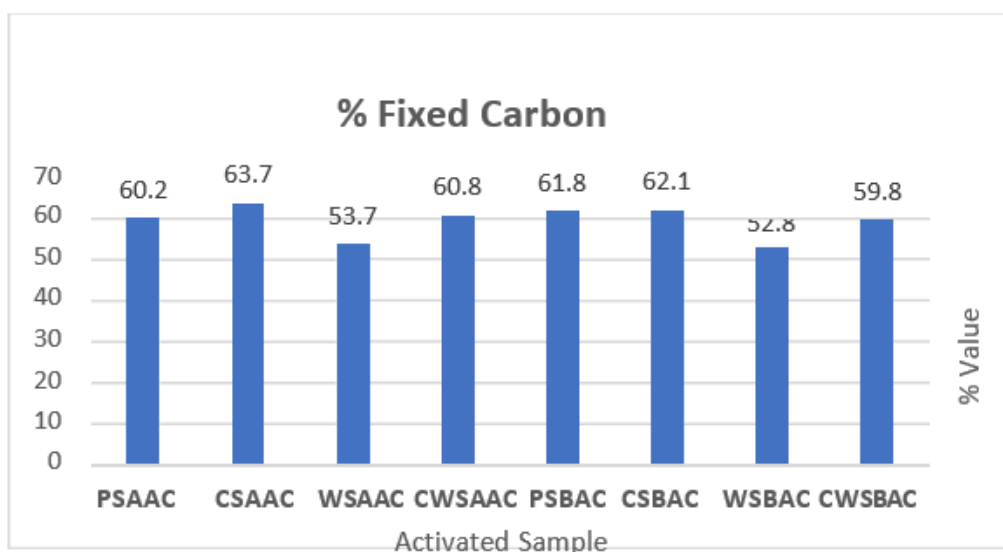


Fig. 6. Fixed carbon yield of acid-activated carbon and base-activated carbon.

3.5 Ash Content

The ash content for the activated samples in Table 5 varied between 7.9% and 12.3%. Acid-activated samples PSAAC, CSAAC, WSAAC, and CWSAAC with values of 7.9, 8.3, 11.8, and 9.8% respectively presented lower ash contents than base-activated samples, with PSAAC having the lowest ash content at 7.9%. This is consistent with the results by [34] in a similar research. In contrast, base-activated samples PSBAC, CSBAC, WSBAC, and CWSBAC presented slightly higher ash contents with values of 8.9, 9.3, 12.3 and 9.9% respectively against that of the acid-activated samples with WSBAC showing the highest at 12.3%. Lower ash content is beneficial for adsorbents as it increases the

available surface area for adsorption and improves overall efficiency.

The activated samples indicate a relatively low percentage ash content which is an indication that the samples will exhibit high adsorptive values. This is because ash is an impurity that reduces the overall activity of the activated carbon. The ash content is very important in determining the quality of an adsorbent with a good adsorbent having as low ash content as possible (<15%) [35]. This is because high ash content reduces the adsorptive capacity of the adsorbent and lowers specific surface area [36]. High ash content also affects the efficiency of the activated samples as the higher the ash content, the lower the efficiency of removal of toxic contaminants.

This is supported by a study by [37] that observed that activated carbon with high ash content adsorbed 4 times less contaminants than ash-free activated carbon.

3.6 Specific Surface Area

The surface area of activated carbon samples typically has a surface area ranging from 500 to 1500 m²/g, making it highly effective for adsorption processes [38]. The carbon samples had a resultant surface area ranging from 960 to 1288m²/g making them suitable for adsorption of PAHs. Comparison between acid and base-activated samples of each crustacean shell sample was noted to vary slightly with the base-activated samples presenting a larger surface area than acid-activated samples. The Surface area for CSBAC and CSAAC are 1288 and 1277 m²/g; PSBAC and PSAAC are 1275 and 1193 m²/g; WSBAC and WSAAC are 986 and 960 m²/g; while CWSBAC and CWSAAC are 1270 and 1256 m²/g respectively. The presence of high surface areas influences adsorption as it presents large active sites for the adhesion of adsorbates from the solution. Carbonization and chemical activation improve the surface area of adsorbents as they improve adsorption sites allowing for more interaction sites between the activated carbon and adsorbate enhancing the adsorption capacity of the activated carbon [39]. [38] noted that the surface area range of activated carbon can vary based on factors such as the activation method used, the precursor material, and the activation conditions during production.

3.7 Bulk Density

Bulk density, also known as apparent density is the mass of activated carbon per unit volume (kg/m³ or g/cm³), including the voids between the particles. Typical powdered activated carbon (PAC) may have a slightly lower bulk density of around 0.38g-0.45g/cm³ than that of a granular activated sample. [40] noted that an activated carbon with a bulk density of about 0.5g/cm³ is adequate for adsorption. The bulk densities of all the crustacean shells activated carbon were found to be within the range of 0.454g/cm³ to 0.687g/cm³. This is similar to results from [41] on the bulk density of low-cost precursors. Usually, adsorbents with high bulk density can hold more adsorbate per unit weight which makes high bulk density essential for wastewater treatment purposes.

3.8 Specific Gravity

The Specific gravity of the activated samples was noted to range from 0.97 observed for WSAAC to 2.01 for CSBAC. This indicates that the activated carbon samples are effective adsorbents for the wastewater treatment process as their ranges conform with the research conducted by [42,43] which stated that the values for the specific gravity of an activated sample lie within the ranges of 0.8 to 2.1.

3.9 Porosity

Table 1 also shows the porosity of the activated carbon samples. Porosity describes the number of pores present in a sample [44]. It can therefore be inferred from this that Porosity enhances the adsorption capacity of an activated carbon sample Therefore the higher the porosity, the higher the adsorption capacity of the adsorbent. It is noted from Table 1 that the porosity of the activated samples is in the order CSBAC (0.88) > PSBAC (0.86) > CSAAC (0.83) > CWSAAC (0.81) > CWSBAC and PSAAC (0.80) > WSAAC (0.62) > WSBAC (0.59).

4. CONCLUSION

The morphology, elemental analysis, physicochemical characteristics, and surface chemistry of chemically activated carbon from crustacean shells were compared. The morphology and physicochemical characteristics of the activated carbons made from periwinkle, clam, whelk, and composite clam/whelk shells are suitable for adsorption, according to the results of the experimental evaluations. Activated carbons with high carbon yield, high fixed carbon, high bulk density, increased surface area, low ash content, low moisture content, and high porosity of carbon were produced by chemical activation methods using both acid and base activation for crustacean shells. These results show that resultant activated carbons are effective as an adsorbent for the industrial treatment of wastewater. With high surface areas of 1288 and 1277 m²/g, respectively, it is reasonable to deduce that clam shells activated with either basic or acid have a better advantage to be used compared to Periwinkle shells, whelk shells, and the composite of clam/whelk shells. This Study revealed that Chemical Activation of Crustacean shells can be undertaken using either acid or base without compromising on the efficiency of the resultant activated sample for the effective removal of

adsorbates from wastewater samples. This therefore expands the choice of activation as the choice of precursors is abundant in nature.

DISCLAIMER (ARTIFICIAL INTELLIGENCE)

Author(s) hereby declare that NO generative AI technologies such as Large Language Models (ChatGPT, COPILOT, etc.) and text-to-image generators have been used during the writing or editing of this manuscript.

COMPETING INTERESTS

Authors have declared that no competing interests exist.

REFERENCES

1. Akomah U, Nwaogazie IL, Akaranta O. A Review on Current Trends in Heavy Metal Removal from Water between 2000-2021. *International Journal of Environment and Climate Change*. 2021;11(12):67-90. DOI: 10.9734/IJECC/2021/v11i1230557
2. Ravenni G, Sárossy Z, Ahrenfeldt J, Henriksen UB. Activity of chars and activated carbons for removal and decomposition of tar model compounds – A review. *Renewable and Sustainable Energy Reviews*. 2015;94:1044-1056. Available: <https://doi.org/10.1016/j.rser.2018.07.001>
3. Zoha H, Mohammad HD, Mohsen H, Gholamali J, Imran A and Mika S. Methods for preparation and activation of activated carbon: a review; 2020. Available: <https://doi.org/10.1007/s10311-019-00955-0>
4. El Gamal M, Mousa HA, El-Naas MH, Zacharia R, Judd S. Bio- regeneration of activated carbon: A comprehensive review. *Separation and Purification Technology*. 2018;197:345-359. Available: <https://doi.org/10.1016/j.seppur.2018.01.015>
5. Ani JU, Akpomie KG, Okoro UC, Aneke LE, Onukwuli OD, Ujam OT. Potentials of activated carbon produced from biomass materials for sequestration of dyes, heavy metals, and crude oil components from aqueous environment. *Appl Water Sci*. 2020;10:69. Available: <https://doi.org/10.1007/s13201-020-1149-8>
6. González-García P. Activated carbon from lignocellulosics precursors: A review of the synthesis methods, characterization techniques and applications. *Renewable and Sustainable Energy Reviews*. 2018; 82:1393-1414. Available: <https://doi.org/10.1016/j.rser.2017.04.117>
7. Ngasotter S, Xavier K, Meitei MM, Waikhom D, Pathak J, Singh SK. Crustacean shell waste derived chitin and chitin nanomaterials for application in agriculture, food, and health – A review. *Carbohydrate Polymer Technologies and Applications*. 2023;6:100349. Available: <https://doi.org/10.1016/j.carpta.2023.100349>
8. Foong SY, Liew RK., Yuh Yek PN, Chan YH, Lam SS. A review in production of nitrogen-enriched carbon materials via chitin pyrolysis and activation for enhanced wastewater remediation. *Current Opinion in Green and Sustainable Chemistry*. 2024;47:100920. Available: <https://doi.org/10.1016/j.cogsc.2024.100920>
9. Topić Popović N, Lorencin V. Shell waste management and utilization: Mitigating organic pollution and enhancing sustainability. *Applied Sciences*. 2020;13(1):623. Available: <https://doi.org/10.3390/app13010623>
10. Hart A. Mini-review of waste shell-derived materials' applications. *Waste Management & Research*. 2020;38(5):514-527. Available: <https://doi.org/10.1177/0734242X19897812>
11. Adeyemi AO, Ojoawo SO. Production and characterization of chitosan of crustacean shells. *Materials Today: Proceedings*. 2022;88:128-134. Available: <https://doi.org/10.1016/j.matpr.2023.05.729>
12. Adedipe O, Medupin R, Yoro K, Dauda E, Aigbodion V, Agbo N, Oyeladun O, Mokwa J, Lawal S, Eterigho-Ikelegbe O, Sadare O. Sustainable carburization of low carbon steel using organic additives: A review. *Sustainable Materials and Technologies*. 2023;38:e00723. Available: <https://doi.org/10.1016/j.susmat.2023.e00723>

13. Sellami A, Elleuch R. Green composite friction materials: A review of a new generation of eco-friendly brake materials for sustainability. *Environmental Engineering Research*. 2023;29(3): 230226.
Available:<https://doi.org/10.4491/eer.2023.226>
14. Magnacca G, Guerretta F, Vizintin A, Benzi P, Valsania MC, Nisticò R. Preparation, characterization and environmental/electrochemical energy storage testing of low-cost biochar from natural chitin obtained via pyrolysis at mild conditions. *Applied Surface Science*. 2017;427: 883-893.
Available:<https://doi.org/10.1016/j.apsusc.2017.07.277>
15. Fapetu OP. Production of charcoal from tropical biomass for industrial and metallurgical process. *Nigerian Journal of Engineering Management*. 2000;1(2):34-37.
16. ASTM D 2866-94, Standard Test Methods for the ash content, ASTM, West Conshohocken, PA.
17. Abate GY, Alene AN, Habte AT, Getahun DM. Adsorptive removal of malachite green dye from aqueous solution onto activated carbon of *Catha edulis* stem as a lowcost bio-adsorbent. *Environmental Systems Research*. 2020;9(1):1-13.
Available:<https://doi.org/10.1186/s40068-020-00191-4>
18. Efevbokhan VE, Alagbe EE, Odika B, Babalola R, Oladimeji TE, Abatan OG, Yusuf EO. Preparation and characterization of activated carbon from plantain peel and coconut shell using biological activators. *J. Phys.: Conf. Ser.* 2019;1378032035.
DOI:10.1088/1742-6596/1378/3/032035
19. Akpan EI, Gbenebor OP, Adeosun SO. Synthesis and characterisation of chitin from periwinkle (*Tympanotonus fusatus* (L.)) and snail (*Lissachatina fulica* (Bowdich)) shells. *International journal of biological macromolecules*. 2018;106:1080-1088.
20. Kunusa WR, Iyabu H, Abdullah R. FTIR, SEM, and XRD analysis of activated carbon from sago wastes using acid modification. In *Journal of Physics: Conference Series*. 2021;1968(1): 012014.
21. Okoya AA, Diisu D. Research Article adsorption of indigo-dye from textile wastewater onto activated carbon prepared from sawdust and periwinkle shell. *Trends in Applied Sciences Research*. 2021;16:1-9.
Available:<http://dx.doi.org/10.3923/tasr.2021.1.9>
22. Eke-emezie N, Etuk BR, Akpan OP, Okechukwu CC. Cyanide removal from cassava wastewater onto H₃PO₄ activated periwinkle shell carbon. *Appl Water Sci*. 2022;12:157.
Available:<https://doi.org/10.1007/s13201-022-01679-3>
23. Heidarinejad Z, Mohammad HD, Mohsen H, Gholamali J, Imran A, Mika S. Methods for preparation and activation of activated carbon: a review. *Environ ChemLett*. 2020;18:393–415.
Available:<https://doi.org/10.1007/s10311-019-00955-0>
Available:<https://www.researchgate.net/publication/279909992>
24. Iwanow M, Tobias G, Volker S and Burkhard K. Activated carbon as catalyst support: precursors, preparation, modification and characterization. *Beilstein J. Org. Chem*. 2020;16: 1188–1202.
Available:<https://doi.org/10.3762/bjoc.16.104>
25. Wang Z, Nie E, Li J, Yang M, Zhao Y, Luo X, Zheng Z. Equilibrium and kinetics of adsorption of phosphate onto iron-doped activated carbon. *Environmental Science and Pollution Research International*. 2011;19(7):2908–2917.
Available:<https://doi.org/10.1007/s11356-012-0799-y>
26. Ramanan G, Dhas JER, Ramachandran M, Samuel GD. Influence of activated carbon particles on microstructure and thermal analysis of aa7075 metal matrix composites. *Rasayan. Journal Chem*. 2017;10(2):375-384.
Available:<http://dx.doi.org/10.7324/RJC.2017.1021663>
27. Wibawa PJ, Nur M, Asy'ari M, Nur H. SEM, XRD, and FTIR analyses of both ultrasonic and heat generated activated carbon black microstructures. *Heliyon*. 2020;6(3): e03546.

- Available:<https://doi.org/10.1016/j.heliyon.2020.e03546>
28. Nabais JMV, Nunes P, Carrott PJ, Carrott MMLR, García AM, Díaz-Díez MA. Production of activated carbons from coffee endocarp by CO₂ and steam activation. *Fuel Processing Technology*. 2008;89(3):262-268. Available:<http://dx.doi.org/10.1016/j.fuproc.2007.11.030>
 29. Ratan JK, Kaur M, Adiraju B. Synthesis of activated carbon from agricultural waste using a simple method: characterization, parametric and isotherms study. *Materials Today: Proceedings*. 2018;5(2):3334-3345. Available:<http://dx.doi.org/10.1016/j.matpr.2017.11.576>
 30. Nworu JS, Ngele SO, Nwabueze E, Okhifo A, Peretomode TM. Quantitative characterization of activated carbon from cow, donkey, chicken and horse bones from Ezzangbo in Ebonyi State, Nigeria. *American Journal of Applied Chemistry*. 2018;6(5):169-174. DOI: 10.11648/j.ajac.20180605.12
 31. Oyedoh EA, Ekesiobi UU. Effects of preparation conditions on surface properties and yields of periwinkle shell activated carbon. *J. Appl. Sci. Environ. Manage*. 2023;27(6):1083-1091. Available:<https://dx.doi.org/10.4314/jasem.v27i6.6>
 32. Kamran M. Energy sources and technologies; 2023. Available:<https://doi.org/10.1016/B978-0-323-99560-3.00010-7>
 33. Akpa JG, Dagde KK. Effect of activation method and agent on the characterization of periwinkle shell activated carbon. *Chemical and Process Engineering Research*. 2018;56. Available:<https://www.iiste.org/Journals/index.php/CPER/article/view/41379>
 34. Gunorubon AJ, Chukwunonso N. Kinetics, equilibrium and thermodynamics studies of Fe³⁺ Ion removal from aqueous solutions using periwinkle shell activated carbon. *Advances in Chemical Engineering and Science*. 2018;8:49-66. Available:<https://doi.org/10.4236/aces.2018.8.2004>
 35. Sabino D, Giusy L, Mariangela G, Michele N. Characteristics and adsorption capacities of low-cost sorbents for wastewater treatment: A review. *Sustainable Materials and Technologies*. 2016;9:10-40. Available:<https://doi.org/10.1016/j.susmat.2016.06.002>
 36. Eke-emezie NC, Etuk BR. Cyanide adsorption from cassava wastewater onto calcined periwinkle shell. *J. Degrade. Min. Land Manage*. 2019;7(1):1929-1934. DOI: 10.15243/jdmlm.2019.071.1929.
 37. Diamadopoulos E, Samaras P, Sakellariopoulos GP. The Effect of Activated Carbon Properties on the Adsorption of Toxic Substances. *Water Science and Technology*. 1992;25(1):153-160.
 38. Ngu LH. Carbon capture technologies. *Encyclopedia of Sustainable Technologies (Second Edition)*. 2023;358-377. Available:<https://doi.org/10.1016/B978-0-323-90386-8.00028-0>
 39. Mopoung S, Nogklai W. Chemical and surface properties of longan seed activated charcoal. *Mopoung, International Journal of Physical Sciences*. 2008;3(10):234-239. Available:<https://doi.org/10.5897/IJPS.9000116>
 40. Okieimen FE, Okieimen CO, Wuana RA. Preparation and characterization of activated carbon from rice husks, *J. of Chem. Soc*. 2007;32:126-136. Available:https://www.researchgate.net/publication/288024125_Preparation_and_characterization_of_activated_carbon_from_rice_husks/citations
 41. Madojemu G, Eze CB, Okieimen F. optimization of surface area of activated carbons prepared from coconut shells by response surface methodology. *Journal of Chemical Society of Nigeria*. 2020;45(2). Available:<https://journals.chemsociety.org.ng/index.php/jcsn/article/view/460>
 42. Boadu KO, Joel OF, Essumang DK, Evbuomwan BO. Comparative studies of the physicochemical properties and heavy metals adsorption capacity of chemical activated carbon from palm kernel, coconut and groundnut shells. *Journal of Applied Sciences and Environmental Management*. 2018;18(1). Available:<https://dx.doi.org/10.4314/jasem.v22i11.19>

43. Hala EG, Sayed AAS, Abdelrahman ST, Abdelazim ME, Karima OA. Adsorption of heavy metals from polluted water using low cost materials. Egyptian Journal of Aquatic Biology and Fisheries. 2019;23(4), 275-284.
Available:<http://dx.doi.org/10.21608/ejabf.2019.54225>
44. Tarawou T, Wankasi D, Horsfall M. Preparation and characterization of activated carbon from water hyacinth (*Eichornia crassipes*) And Water Spinach (*Ipomoea aquatica*). Scientia Africana. 2011;10(1):21-27.
Available:<https://www.ajol.info/index.php/sa/article/view/156656/146263>

Disclaimer/Publisher's Note: The statements, opinions and data contained in all publications are solely those of the individual author(s) and contributor(s) and not of the publisher and/or the editor(s). This publisher and/or the editor(s) disclaim responsibility for any injury to people or property resulting from any ideas, methods, instructions or products referred to in the content.

© Copyright (2024): Author(s). The licensee is the journal publisher. This is an Open Access article distributed under the terms of the Creative Commons Attribution License (<http://creativecommons.org/licenses/by/4.0>), which permits unrestricted use, distribution, and reproduction in any medium, provided the original work is properly cited.

Peer-review history:

The peer review history for this paper can be accessed here:

<https://www.sdiarticle5.com/review-history/123527>